

Article

Not peer-reviewed version

---

# Effects of Humic Acid From Weathered Coal on Water-Stable Aggregates and Pore Structure of a Reclaimed Cambisol

---

Xiaoying Di , [Wenhua Fan](#) <sup>\*</sup> , Qinghui Meng , [Fenwu Liu](#) , Gailing Wang

Posted Date: 16 July 2024

doi: 10.20944/preprints202407.1324.v1

Keywords: reclaimed cambisol; humic acid; water-stable aggregate; soil pore



Preprints.org is a free multidiscipline platform providing preprint service that is dedicated to making early versions of research outputs permanently available and citable. Preprints posted at Preprints.org appear in Web of Science, Crossref, Google Scholar, Scilit, Europe PMC.

Copyright: This is an open access article distributed under the Creative Commons Attribution License which permits unrestricted use, distribution, and reproduction in any medium, provided the original work is properly cited.

Article

# Effects of Humic Acid from Weathered Coal on Water-Stable Aggregates and Pore Structure of a Reclaimed Cambisol

Xiaoying Di <sup>1,2</sup>, Wenhua Fan <sup>1,\*</sup>, Qinghui Meng <sup>1</sup>, Fenwu Liu <sup>1</sup> and Gailing Wang <sup>1</sup>

<sup>1</sup> College of Resources and Environment, Shanxi Agricultural University, Jinzhong 030801, China; dixiaoying@jzci.edu.cn; liufenwu@sxau.edu.cn (F.L.); 13233054308@163.com (G.W.); mengqinghui9897@163.com (Q.M.);

<sup>2</sup> College of Food and Environment, Jinzhong College of Information, Jinzhong 030801, China;

\* Correspondence: fwh012@163.com; Tel.15835443728;

**Abstract:** To clarify effects of weathered coal humic acid on water-stable aggregates and pore characteristics of reclaimed cambisol, this research analyzed the evolution characteristics of soil aggregates and pores. Effects of different humic acid dosages (0, 1%, 3%, and 5% by weight) and application period (1 year, 2 years, and 3 years) on soil aggregates and organic carbon components in soil water-stable aggregates were investigated. The results showed that water-stable macroaggregates (>0.25 mm) had the highest content in the first year; but in the third year, water-stable microaggregates (0.053–0.25 mm) had the highest content, and silt and clay (<0.053 mm) were at a maximum. In the third year of 5% treatment, mean weight and geometric mean diameters were the largest, soil structure was the most stable, and TOC and water-stable microaggregates (0.053–0.25 mm) in soil had the highest proportions. For 5% treatment, the majority of irregular pores were independent in the first year, and number of pores decreased in the second year, but average pore volume increased, forming robust connected pores. In the third year, the number of elongated and irregular pores increased. In the third year of 5% treatment, most pores were irregular and of size >100  $\mu\text{m}$ , and soil structure was the most stable.

**Keywords:** reclaimed cambisol; humic acid; water-stable aggregate; soil pore

## 1. Introduction

Soil structure is the spatial arrangement of soil solids and pores, with soil aggregates the basic units making up soil structure [1]. Soil pores are the concrete embodiment of soil structure, with the more soil pores are divided, the more complex is soil structure [2]. According to the hierarchical theory of the formation of soil aggregates, soil pores exist not only among but also inside aggregates. On the one hand, the hydrophobic property of soil solids ensures the infiltration and penetration of soil water into soil pores, which increases the stability of soil structure. On the other hand, soil pores are also important sites for activities of soil microbial communities, which play an important role in the soil carbon (C) cycle [3]. With the development of three-dimensional imaging, soil pore structure acquisition technology has a wide application prospect because of its greatly simplified procedures, especially CT scanning technology, which reflects the internal pore structure of soil in a non-destructive and intuitive way with three-dimensional images [4], and tends to make the understanding of soil function “transparent” [5].

When land reclamation is carried out in coal mining subsidence areas, the use of heavy machinery and other reclamation measures causes problems of poor structure and low nutrient content of reclaimed soil [6–8], and rapid improvement of reclaimed soil quality has become a key issue. Humic acid from weathered coal contains a variety of oxygen-containing functional groups—including carboxyl, carbonyl, phenolic hydroxyl, alcohol hydroxyl, enol, methoxy, sulfonic, quinone,

and ketone groups—which can better promote the agglomeration of soil particles to form aggregate structure, increase the content and stability of water-stable aggregates [9], and improve ventilation permeability. As a soil conditioner [10], weathered coal humic acid can improve soil quality, transform barren soil and saline-alkali soil, promote soil microorganism and enzyme activity, and increase the utilization rate of phosphate fertilizer. Current research mainly focuses on the effects of weathered coal humic acid on soil nutrients, soil microorganisms [11], crops, and saline-alkali land improvement, and few studies have considered its improvement of soil structure, especially the reclaimed cambisol structure.

In view of the above, based on a 3-year reclamation soil micro-plot experiment, this study analyzed the influence of weathered coal humic acid on the aggregate distribution and soil pore structure of reclaimed cambisol with the help of CT scanning technology, explored the relationship of weathered coal humic acid with the structural evolution of reclaimed cambisol and the improvement of soil quality, and provided a theoretical basis for the application of humic acid in improving the structure of reclaimed soil.

## 2. Materials and Methods

### 2.1. Study Site and Soil Properties

The experiment was established on the reclamation base of Xiangyuan Coal mine area located at Xiangyuan City (36° 28'N, 113° 00'E, average altitude 1050 m), Changzhi, Shanxi Province, China. This base was reclaimed by filling (i.e. mixed pushing) in 2008. The region has a warm temperate semi-humid continental monsoon climate with average annual temperature of 9.5 °C, average annual precipitation of about 550 mm, 60–70% of precipitation concentrated from July to September, and a frost-free period generally of 150–166 days. The soil in this area is mainly Calcaric Cambisol and loess parent material. Before initiating the experiment, the soil with pH 8.20 contained 8.62 g organic C/kg, 15.26 mg alkali-N/kg, 4.57 mg Olsen P/kg, and 91.73 mg available K/kg.

The weathered coal humic acid was provided by Shanxi Jiaocheng Hongxing Chemical Co., Ltd., comprising black powder with organic matter content of 615.81 g/kg and humic acid content of 37.34%

### 2.2. Experiment Design

A 3-year field micro-plot experiment was started on May 21, 2019. Four treatments were set up: CK: no addition of weathered coal humic acid, 1% treatment: the addition of weathered coal humic acid equal to 1% of the weight of the surface soil (i.e., 1% by weight); 3% treatment: the addition of weathered coal humic acid equal to 3% of the weight of the surface soil; and 5% treatment: the addition of weathered coal humic acid equal to 5% of the weight of the surface soil. Three replicates were taken from different treatments at each testing site according to random block design every year. The every treatment (e.g.: 1%, 3%, 5%) had 9 micro-plots respectively, and CK treatment had 3 micro-plots. There were 30 micro-plots in total. The micro-plots were 1 m × 1 m, and each had a surrounding ridge about 20 cm wide. When the weathered coal humic acid (sieved through a 2-mm sieve) was added, it was necessary to artificially mix it with the soil evenly, smooth the surface, and no crops were planted. Samples were collected before adding the weathered coal humic acid at 1 and 2 years (i.e., years 1 and 2), and only samples without added weathered coal humic acid were collected at 3 years (year 3). During sampling, 1%, 3%, 5%, and CK treatments were randomly selected, each treatment was replicated three times, and 12 samples were collected each time.

### 2.3. Soil Sampling

For the determination of soil organic C, fresh soil samples were taken from eight randomly selected cores in each plot at 0–20 cm depth, and thoroughly mixed to form a composite sample. The visible soil impurities (e.g., stones, organic debris, and plant residues) were carefully removed with forceps, samples were dried with natural air after passing through 1mm, 2mm, and 0.149mm soil sieves, and then used for determination of soil organic C.

Undisturbed soil samples were collected for aggregate separation. To avoid the undisturbed soil samples being crushed, they were packed into large aluminum boxes and taken back to the laboratory. The distribution of aggregates, particulate organic C (POC), and mineral bound organic C (MOC) were determined by wet-sieving method.

Undisturbed soil columns were collected for pore character analysis. A PVC rigid pipe with an inner diameter of 50 mm, thickness of 2 mm, and length of 100 mm was used for collection, and one sample was collected for each micro-plot. Before sampling, one end of the PVC pipe was sharpened into a knife edge for sampling. Finally, both ends of the PVC pipe were wrapped with plastic wrap, covered with a cap, and placed vertically in an insulated box to ensure integrity of the soil column during transportation and scanning. After returning to the laboratory, samples were stored in a refrigerator at 4 °C.

Soil samples were obtained in June 2020, 2021, and 2022. The PVC cores from the 0–20 cm layer in every micro-plot and soil samples were immediately delivered to the laboratory and manually divided into two parts. One was air-dried for further experiments, such as soil aggregate fractionation (within one week), and the other part passed through sieves for physicochemical determination.

#### 2.4. Laboratory Analysis

Wet-sieving method was used for classifying aggregates. Organic C concentrations of the bulk soils, aggregates, and density fractions were determined by the wet oxidation–redox titration method. Soil POC and MOC were obtained by sodium hexametaphosphate dispersion [12].

The stability of soil aggregates was expressed by mean weight diameter (MWD) and geometric mean diameter (GMD), with the formulas as follows:

$$MWD = \sum_{i=1}^n (\bar{X}_i W_i) \quad (1)$$

$$GMD = \exp \left( \frac{\sum_{i=1}^n W_i \lg X_i}{\sum_{i=1}^n W_i} \right) \quad (2)$$

where  $X$  represents the mean diameter of the aggregate with the size class (mm),  $W$  is the proportion of the mass of the size class aggregate to the total mass of the soil tested (%), and  $n$  is the number of sievings.

The pore structure of soil was scanned by Phoenix Industrial X-ray CT scanner (Nanotom S) in the Institute of Soil Research, Chinese Academy of Sciences, and Image J software was used to reconstruct the image and obtain the characteristic parameters of the pore structure [13]. The total porosity, pore number and were calculated with the '3d object counter' plugin in the Image J.

Pore shapes are generally divided into three types, according to  $F$ : elongated ( $F \leq 0.2$ ), irregular ( $0.2 < F < 0.5$ ), and regular shapes ( $F \geq 0.5$ ) [14]. The proportion of the three shapes is calculated by the number of pores. The pore size distribution is based on the equivalent diameter ( $P$ ) of soil pores, which divides soil pores into micropores ( $P_{<30\mu\text{m}}$ ), mesopores ( $P_{30-75\mu\text{m}}$ ), macropores ( $P_{75-100\mu\text{m}}$ ), and ultramacropores ( $P_{>100\mu\text{m}}$ ) [15]. The soil pore shape factor ( $F$ ) describes a specific surface as the ratio of total pore surface area to aggregate volume. In this study,  $F$  is an index representing the pore shape, calculated using the following formula:

$$F = A_e/A \quad (3)$$

where  $A_e$  is the surface area of a sphere, equal to the pore volume; and  $A$  is the pore surface area. When  $F = 1$ , the pores are round; when  $F < 1$ , pore shape is more irregular.

Mean pore volume, Pore number, connected pore number, disconnected pore number and connectivity were determined using the 'Bong J plugin [14]. Usually, the degree of anisotropy (DA) can be used to represent the porosity roundness,

## 2.5. Statistics Analysis

The results are expressed as mean  $\pm$  standard deviation. One-way ANOVA was used to determine significant differences in soil properties and pore characteristics in reclaimed cambisol with different levels of weathered coal humic acid. Where significant differences between the means were noted, Duncan's test was performed at  $P < 0.05$ . All statistical analyses and graphing were conducted with Image J, SPSS 19.0 (SPSS Inc., Chicago, IL, USA) and Origin 2024, respectively (Origin Lab Inc., Northampton, MA, USA).

## 3. Results

### 3.1. Influence of Humic Acid on Distribution and Stability of Water-Stable Aggregates

#### 3.1.1. Distribution of Water-Stable Aggregates

Figure 1 shows the distribution of water-stable aggregates. In the same year, the water-stable macroaggregates ( $>0.25$  mm) were the majority, followed by water-stable microaggregates (0.053–0.25 mm), and the last was silt and clay ( $<0.053$  mm). The water-stable large aggregates increased with the increased application of weathered coal humic acid for years 1 and 3, but decreased for year 2; the lowest value was 39.16% under 5% treatment. In contrast to the large water-stable aggregates, the water-stable microaggregates decreased with increased application of humic acid for years 1 and 3, and then increased for year 2. The silt and clay increased with increasing application of weathered coal humic acid. Within the same treatment, the water-stable macroaggregates initially decreased and then increased with time, while water-stable microaggregates and silt and clay consistently increased.

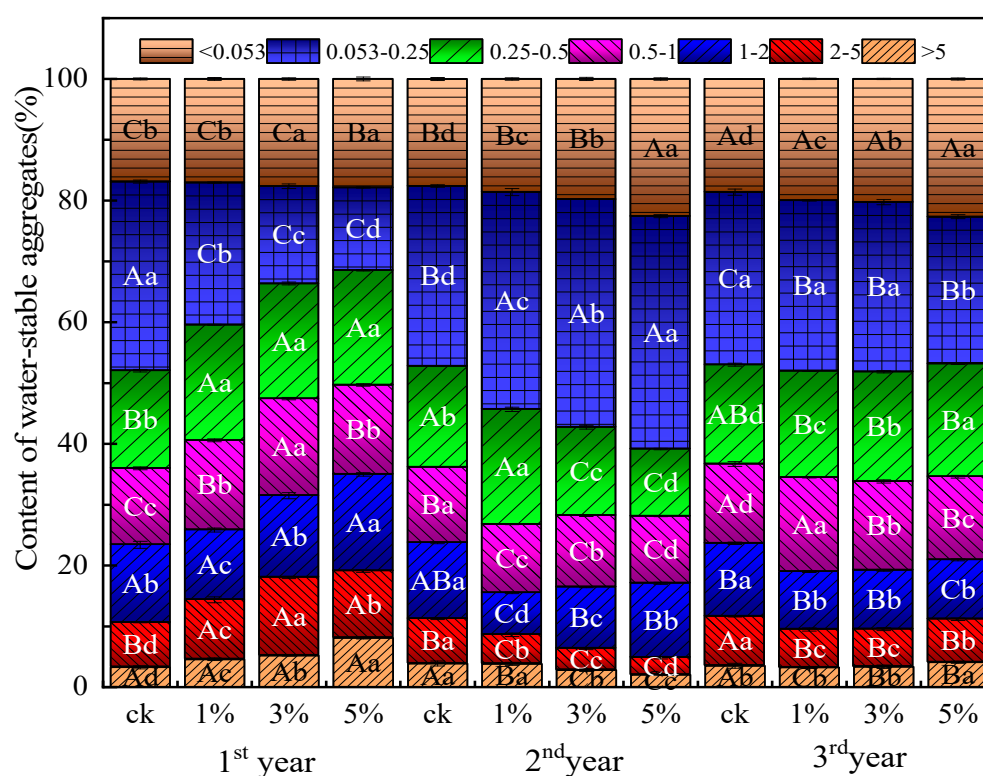


**Figure 1.** Distribution of water-stable aggregates in reclaimed cambisol for different weathered coal humic acid treatments in years 1–3. Note: Different lowercase letters indicate, for the same aggregate fraction and the same age, significant differences in the proportion of water-stable aggregates between treatments ( $P < 0.05$ ); different uppercase letters indicate, for the same aggregate fraction and the same

treatment, significant differences in the proportion of water-stable aggregates between years ( $P < 0.05$ ).

For year 1, there was no significant difference in water-stable aggregates  $>5$  mm; but that of 2–5 mm was significantly increased compared with CK ( $P < 0.05$ ). When accounting for all fractions, water-stable aggregates was highest in the 3% treatment, with an increase of 5.51% compared with the CK. Water-stable aggregates of 1–2 mm increased with increased humic acid application; however, there was no significant difference among treatments ( $P < 0.05$ ). Water-stable aggregates of 0.5–1 mm for each treatment was significantly increased compared with CK ( $P < 0.05$ ), and the 3% treatment had the largest increase, reaching 15.47%. Water-stable aggregates of 0.25–0.5 and 0.053–0.25 mm for each treatment were significantly decreased compared with CK ( $P < 0.05$ ), which only accounted for 18.85% and 13.63% of all fractions in the 5% treatment, respectively. And  $<0.053$  mm increasing with the amount of humic acid was a maximum of 17.84% in the 5% treatment. In contrast to year 1, water-stable macroaggregates at year 2 decreased with increased application of humic acid. Water-stable aggregates of 0.25–0.5 mm in the 5% treatment decreased by 33.54%, and water-stable microaggregates and silt and clay were the highest in the 5% treatment with 17.49% and 29.31%, respectively, and significantly differed from other treatments ( $P < 0.05$ ). The water-stable microaggregates decreased for years 1 and 3, and the greatest decrease was in the 5% treatment with 21.79%. Water-stable aggregates of the silt and clay fraction increased with increased humic acid application, and were greatest for the 5% treatment with 22.65%, and significantly differed from other treatments ( $P < 0.05$ ).

### 3.1.2. Stability of Water-Stable Aggregates

Aggregate stability was affected by the year and the amount of humic acid application (Table 1). The MWD and GMD were affected by the year and the amount of humic acid application, and the maxima for the 5% treatment for the 3 years were 3.91 and 1.62 mm, respectively. Among them, MWD was positively correlated with year, which was significantly higher by 84.43% at year 3 compared with year 2 ( $P < 0.05$ ). The GMD in the same year was significantly higher compared with CK ( $P < 0.05$ ), and the 5% treatment for year 3 had the largest increase compared with CK, reaching 78.02%, and was significantly higher compared with year 2 ( $P < 0.05$ ), with an increase of 0.86 mm. Therefore, aggregates of reclaimed cambisol were the most stable under 3% treatment.

**Table 1.** MWD and GMD of water-stable aggregates for reclaimed cambisol following weathered coal humic acid treatment for years 1–3.

Treatments	MWD/mm			GMD/mm		
	1st year	2nd year	3rd year	1st year	2nd year	3rd year
CK	1.22 ± 0.08Ba	1.44 ± 0.19Ba	1.55 ± 0.21Ca	0.4 ± 0.02Bb	0.39 ± 0.09Bb	0.91 ± 0.21Ba
1%	1.06 ± 0.07Bb	1.56 ± 0.2Ba	1.7 ± 0.13Ca	0.49 ± 0.19Ab	0.66 ± 0.08ABb	0.87 ± 0.25Ba
3%	1.3 ± 0.06Bb	1.72 ± 0.11Abb	2.43 ± 0.18Ba	0.49 ± 0.15Aa	0.72 ± 0.11Aa	0.54 ± 0.02Ca
5%	1.81 ± 0.22Ab	2.12 ± 0.11Ab	3.91 ± 0.05Aa	0.59 ± 0.11Aab	0.76 ± 0.08Ab	1.62 ± 0.12Aa

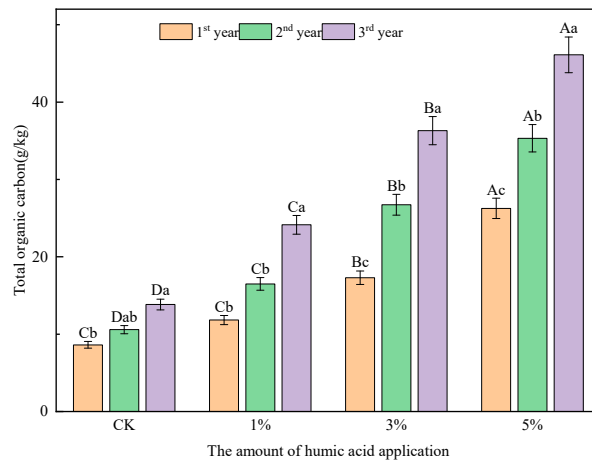
Note: The data in the table are averages ± standard errors; different capital letters in the same column of data indicate significant difference among treatments for the same age ( $P < 0.05$ ); lowercase letters of different peer data indicate significant differences for the same treatment and different years ( $P < 0.05$ ), the same below.

## 3.2. Influence of Weathered Coal Humic acid on Soil Organic C

### 3.2.1. Total Organic C (TOC) of Reclaimed Cambisol

The TOC content of reclaimed cambisol was positively correlated with years and weathered coal humic acid application (Figure 2). Within the same year, the highest organic C content was for the 5% treatment, which was significantly higher than CK ( $P < 0.05$ ). The maximum increase was 32.26 g/kg in the 3 years compared with CK. Under the same treatment, organic C content was the highest

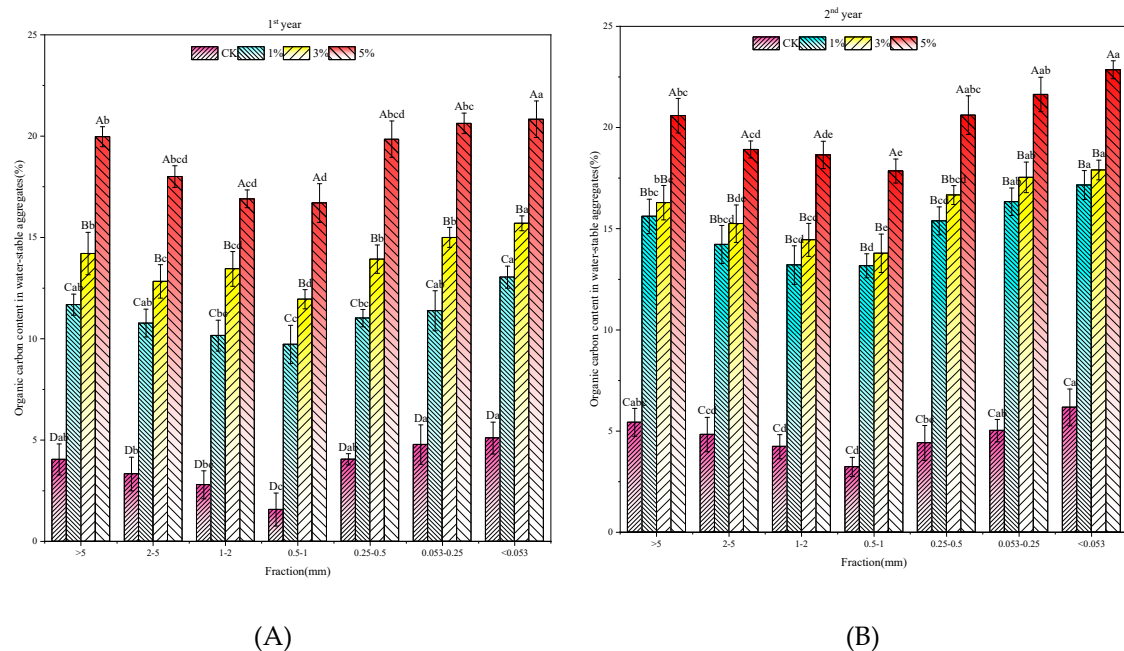
for 5% treatment at year 3, with 46.10 g/kg, an increase of 19.84 g/kg compared with year 1, and the difference among years was significant ( $P < 0.05$ ).



**Figure 2.** Total organic carbon content of reclaimed cambisol under different weathered coal humic acid treatments for years 1–3.

### 3.2.2. Organic C in Water-Stable Aggregates

The organic C content of water-stable aggregates of each treatment presented a state of “higher on both sides and lower in the middle” with the decreasing of aggregate fraction in the same year (Figure 3), and the aggregate fraction content of 0.5–1 mm was the lowest, which significantly increased in each treatment compared with CK ( $P < 0.05$ ), among which, the 5% treatment was 15.00 g/kg greater than for CK. For the same aggregate fraction, the organic C content of water-stable aggregates in different treatments was positively proportional to the application amount, with significant differences among treatments compared with CK ( $P < 0.05$ ).



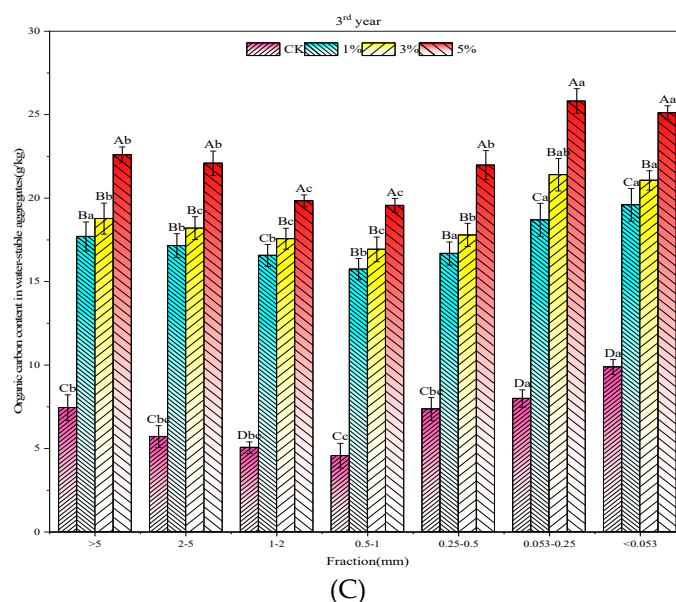


**Figure 3.** Organic carbon content in water-stable aggregates of reclaimed cambisol for different weathered coal humic acid treatments. Note: Different lowercase letters indicate significant differences in organic carbon of water-stable aggregates of different fractions under the same treatment ( $P < 0.05$ ); different capital letters indicate significant differences in organic carbon among water-stable aggregates of the same fraction and different treatments ( $P < 0.05$ ).

For year 1, there were significant differences among all treatments and between all treatments and CK ( $P < 0.05$ ). For year 2, there were no significant differences between 1% and 3% treatments; however, there were significant differences in all treatments compared with CK ( $P < 0.05$ ). At year 3, there was no significant difference between 3% and 1% treatments except for the 1–2 mm fraction in soil large aggregates ( $>0.25$  mm) ( $P < 0.05$ ). The soil microaggregates (0.053–0.25 mm) and silt and clay ( $<0.053$  mm) significantly differed from the 1% treatment to 3% treatment ( $P < 0.05$ ). In the same treatment, the organic C content of the  $<0.053$  mm fraction was the highest for years 1 and 2, and there was a significant difference between the aggregate fraction of the 5% treatment and other aggregate fractions at year 1 ( $P < 0.05$ ); there was a significant difference between the 5% treatment and CK at year 2 ( $P < 0.05$ ), and its highest value was 22.85 g/kg. However, the difference between year 3 and other years was that the 0.053–0.25 mm water-stable aggregates of 3% and 5% treatments had higher organic C content, and the difference between the 5% treatment (with the highest organic C content of 20.40 g/kg) and CK was significant ( $P < 0.05$ ).

### 3.2.3. POC and MOC Contents in Soil Aggregates

The content of POC and MOC in soil aggregates show in Table 2. Among different treatments in the same year, POC content of 0.25–0.5 mm was highest for the 5% treatment. The maximum MOC content was for 0.25–0.5 mm at the 1st year, and for  $<0.053$  mm in the 2nd and 3rd years, while the maximum MOC content for  $<0.053$  mm was 13.82 g/kg in the 3rd year. The variation range of POC of 0.25–0.5 mm for the 5% treatment was 12.42–16.05 g/kg, and the range of MOC content for  $<0.053$  mm was 11.58–15.58 g/kg. The maximum range for the 5% treatment content was in year 1, with POC of 4.40–12.42 g/kg and MOC of 6.2–11.85 g/kg; the content for 0.25–0.5 mm was high for years 2 and 3, and the maximum was for year 3, with significant difference compared with year 1 humic acid treatment in different years.

**Table 2.** Contents of POC and MOC in reclaimed cambisol under different weathered coal humic acid treatments for years 1–3.

Treatments	Fraction	POC(g/kg)			MOC(g/kg)		
		1st year	2nd year	3rd year	1st year	2nd year	3rd year

		(mm)						
CK	>5	2.03 ± 0.6Ab	3.38 ± 0.94Ab	3.08 ± 0.93Ab	2.19 ± 0.37Ac	3.62 ± 1.03Ac	3.64 ± 1.09Ac	
	2-5	2.17 ± 0.51Bc	3.50 ± 0.73ABb	4.77 ± 1.29Ac	2.80 ± 0.92Bb	4.09 ± 0.51Ac	4.96 ± 0.27Ab	
	1-2	5.5 ± 0.7Bb	6.41 ± 1.07Bb	7.35 ± 0.45Ac	6.87 ± 0.54Bb	8.19 ± 0.74Ab	9.96 ± 0.88Ab	
	0.5-1	6.3 ± 1.06Bb	7.21 ± 1.28ABb	9.31 ± 1.03Ab	9.58 ± 0.88Aa	10.19 ± 0.46Ab	10.41 ± 0.69Ab	
	0.25-0.5	7.77 ± 0.5Ac	8.23 ± 0.96Ac	9.46 ± 0.92Ab	5.18 ± 0.63Bd	6.94 ± 0.8Ac	8.1 ± 0.63Ab	
	0.053-0.25	1.7 ± 0.4Ab	2.48 ± 1.12Ac	3.11 ± 1.02Ac	3.41 ± 1.03Bb	4.83 ± 0.44Bb	7.54 ± 0.85Ab	
	<0.053	1.74 ± 0.94Bd	3.32 ± 0.86ABc	4.47 ± 1.43Ad	2.75 ± 1.03Bc	3.78 ± 0.3Bc	5.77 ± 0.62Ac	
1%	>5	2.59 ± 0.69Bab	3.25 ± 0.28Ab	3.69 ± 0.82ABb	1.84 ± 0.63Bc	4.48 ± 1.03Abc	4.4 ± 0.86Abc	
	2-5	6.07 ± 0.85Bb	9.62 ± 0.94Aa	7.64 ± 0.55Abc	4.37 ± 1.28Cb	5.02 ± 1.15Bc	5.91 ± 0.58Bb	
	1-2	6.1 ± 0.82Bb	7.47 ± 1.09Bb	9.72 ± 0.72Ab	7.63 ± 1.14Aa	8.66 ± 1.04Ab	9.7 ± 0.86Ab	
	0.5-1	7.86 ± 1.23Ab	8.19 ± 1.14Ab	9.62 ± 0.69Ab	8.25 ± 0.79Ba	11.02 ± 0.78Ab	12.00 ± 1.8Aab	
	0.25-0.5	9.38 ± 0.54Bb	10.53 ± 0.7ABb	11.28 ± 1.16Ab	6.83 ± 0.59Cc	9.37 ± 1.19Bb	12.55 ± 0.83Aa	
	0.053-0.25	2.36 ± 0.24Bb	4.96 ± 0.55Ab	5.75 ± 0.84Ab	4.73 ± 0.87Ab	6.43 ± 1.39Ab	6.57 ± 0.5Ab	
	<0.053	3.84 ± 0.54Bc	4.66 ± 0.78Bc	6.65 ± 1.03Ac	5.84 ± 1.11Ab	6.79 ± 1.53Ab	7.23 ± 1.04Abc	
3%	>5	3.2 ± 1.25Aab	4.21 ± 0.66ABab	3.81 ± 0.81Ab	3.32 ± 1.02Bb	4.89 ± 1.01Aab	5.06 ± 1.28Aab	
	2-5	8.12 ± 1.47Aa	10.1 ± 0.37Aa	9.26 ± 0.98Aab	8.61 ± 0.45Aa	9.10 ± 0.98Ab	10.1 ± 0.52Ab	
	1-2	7.86 ± 1.14Aa	6.66 ± 0.63Ab	6.82 ± 1.08Ac	6.09 ± 0.76Ca	7.75 ± 0.62Bb	9.28 ± 0.82Ab	
	0.5-1	7.85 ± 1.53Ab	8.37 ± 1.04Ab	9.67 ± 0.89Ab	8.87 ± 0.36Ba	11.22 ± 1.08Ab	12.5 ± 1.27Aab	
	0.25-0.5	10.6 ± 0.62Ab	10.94 ± 0.43Ab	11.39 ± 1.15Ab	9.89 ± 0.8Bb	11.68 ± 0.76ABa	12.55 ± 1.13Aa	
	0.053-0.25	2.62 ± 0.56Bb	5.06 ± 0.23Ab	5.6 ± 0.84Ab	4.71 ± 0.49Bb	6.58 ± 1.42Ab	7.77 ± 0.17Ab	
	<0.053	5.89 ± 0.84Bb	7.56 ± 1.3ABb	8.81 ± 1.11Ab	7.45 ± 1.19Ab	7.16 ± 0.89Ab	7.8 ± 0.65Ab	
5%	>5	4.4 ± 1.18Ba	5.54 ± 0.88Ba	6.17 ± 1.1Ba	6.2 ± 0.59ABc	6.36 ± 0.32Aa	7.62 ± 0.94Aa	
	2-5	8.8 ± 1.06Aa	10.55 ± 1.1Aa	10.32 ± 1.12Aa	8.34 ± 1.21Ba	10.30 ± 1.1Ba	10.64 ± 0.75Aa	
	1-2	9.1 ± 0.44Ba	11.24 ± 1.01Aa	11.9 ± 0.67Aa	10.59 ± 0.97Aa	10.86 ± 0.62Aa	12.09 ± 0.99Aa	
	0.5-1	10.59 ± 0.85Aa	11.49 ± 0.93Aa	11.81 ± 1.31Aa	9.62 ± 0.77Ba	13.54 ± 1.12Aa	13.82 ± 0.62Aa	
	0.25-0.5	12.42 ± 1.09Ba	13.35 ± 0.99Ba	16.05 ± 0.86Aa	11.85 ± 0.3Ba	13.42 ± 0.91Aa	13.44 ± 0.67Aa	
	0.053-0.25	4.89 ± 0.78Ba	8.45 ± 1.28Aa	9.33 ± 0.71Aa	10.73 ± 0.86Ba	12.4 ± 0.55Aa	13.83 ± 1.49Aa	
	<0.053	9.37 ± 0.7Ba	9.92 ± 0.84ABa	11.35 ± 0.63Aa	11.58 ± 0.47 Ba	13.63 ± 1.28ABa	15.58 ± 1.19Aa	

### 3.3. Influence of Weathered Coal Humic Acid on Soil Pore Structure

Application years affected the pore structure parameters of soil treated with weathered coal humic acid (Table 3). In 3rd year, total porosity of reclaimed cambisol under the 5% treatment was the highest, which significantly differed from CK ( $P < 0.05$ ).

Anisotropy changes in this study were not large, which were greater than 1, indicating that horizontal pores mainly existed. After the 2nd year, the increase of soil pore anisotropy decreased, and soil permeability basically stabilized. The number of soil pores reached its maximum in the 3rd year, which was significantly greater than for other years ( $P < 0.05$ ).

The average pore volume of reclaimed cambisol was the maximum in the 2nd year, and it was decreased by 27.00% in the 3rd year. In the 2nd year, pores in soil for 5% treatment were mainly thick and interconnected, with a small number of pores and large average volume. In year 3, some pores were broken and fractured to form fine pores. In year 1, pore connectivity was lower than in year 2.

**Table 3.** Pore structure parameters in reclaimed cambisol under different weathered coal humic acid treatments for years 1–3.

Year	Treatments	Total porosity /%	Degree of Anisotropy	Connective pore number / $\times 10^3$	Disconnective pore number / $\times 10^3$	Pore number / $\times 10^3$	Mean pore Volume / $\times 10^3$	Connectivity /%
1	CK	0.17±0.03c	1.53±0.07a	4.60±0.04b	5.85±0.67b	5.40±0.54d	3.65±0.47c	15.57±0.25b
1	5%	0.43±0.01abc	1.60±0.43a	6.02±0.7b	7.49±0.32b	10.90±0.93cd	6.18±0.43cd	15.46±0.41b
2	CK	0.33±0.34b	1.39±0.18a	4.19±0.90b	6.12±0.11b	6.69±0.52cd	4.23±0.68c	9.41±0.90b
2	5%	0.44±0.02ab	1.69±0.32a	6.15±0.96b	6.49±0.80b	14.24±0.12b	15.85±0.69a	36.56±0.42a
3	CK	0.37±0.04ab	1.60±0.10a	8.09±0.36a	6.91±0.34b	7.82±0.79cd	7.34±0.95cd	15.91±1.01b
3	5%	0.48±0.03a	1.70±0.10a	12.02±0.77a	21.79±0.67a	22.52±1.08a	11.57±0.71ab	23.07±1.26b

### 3.3.1. Soil Pore Shape and Distribution

The most irregular pores existed in the reclaimed cambisol for weathered coal treatment, followed by regular pores and finally fine pores (Figure 4). The proportion of thin and irregular pores increased with time, while the proportion of regular pores decreased. In the 3rd year, the irregular pores under 5% treatment were the most, reaching 75.27%. This conclusion is consistent with soil pore three-dimensional morphology.

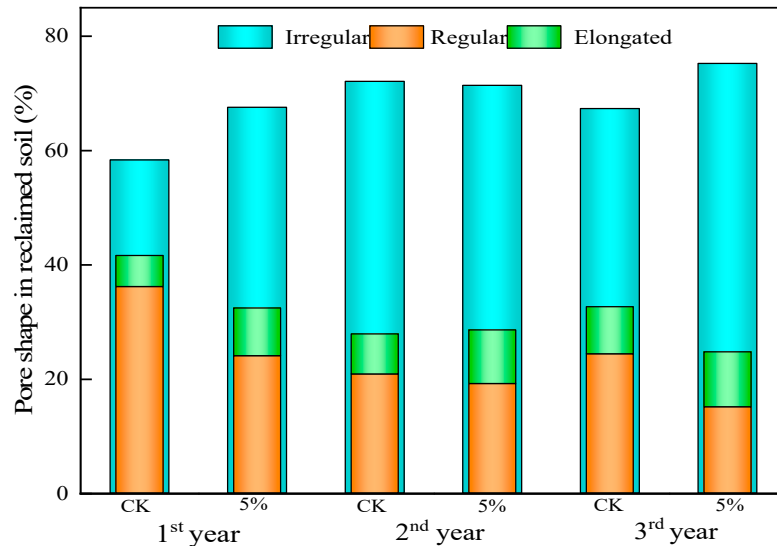


**Figure 4.** Pore shape of reclaimed cambisol treated with 5% weathered coal humic acid.

The quantity of  $P_{30-75\mu\text{m}}$  in the 5% treatment decreased with time, while the quantity of  $P_{75-100\mu\text{m}}$  and  $P_{>100\mu\text{m}}$  increased (Figure 5). The pore quantity of  $P_{30-75\mu\text{m}}$  and  $P_{>100\mu\text{m}}$  in CK increased with time, while  $P_{75-100\mu\text{m}}$  decreased; the quantity of  $P_{>100\mu\text{m}}$  decreased first and then increased slightly with time; the number of  $P_{>100\mu\text{m}}$  was highest, followed by  $P_{30-45\mu\text{m}}$ , and the least was  $P_{75-100\mu\text{m}}$ . Differing from CK, the quantity of  $P_{30-45\mu\text{m}}$  in the 5% treatment decreased with time, but the quantity of  $P_{75-100\mu\text{m}}$  and  $P_{>100\mu\text{m}}$  increased; at year 3,  $P_{>100\mu\text{m}}$  and  $P_{75-100\mu\text{m}}$  reached the highest values (58.4% and 19.7%, respectively), while  $P_{30-45\mu\text{m}}$  had the lowest value (21.9%).

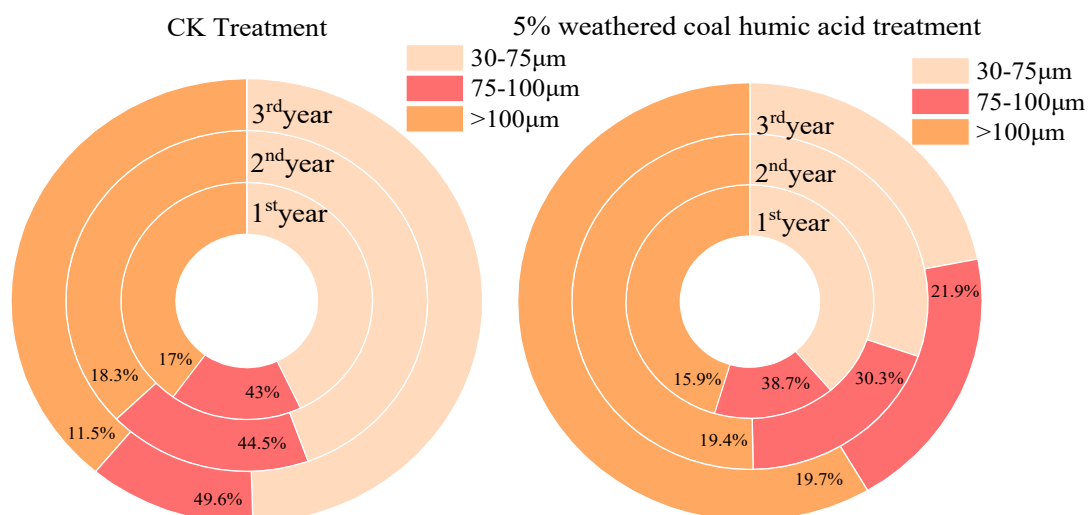


**Figure 5.** Pore distribution in reclaimed cambisol under 5% weathered coal humic acid treatment from the 1st year to the 3rd year.

### 3.3.2. Three-Dimensional Morphological Characteristics of Soil Pores

There were more pores in the soil with 5% treatment in year 3 than in other years (Figure 6). The number of connected pores increased, the number of large pores increased, and a relatively perfect “pore network” was formed.

In year 1, compared with CK with fewer sporadic pores, the number of pores increased significantly under the 5% treatment, pores of different sizes appeared, and local larger pores gradually developed. In year 2, the number of soil pores increased significantly, but small pores still dominated, and large pores continued to develop, while the number of large pores increased under the humic acid treatment. In year 3, the number of pores continued to increase and the distribution was more uniform, but the distribution of larger pores showed new characteristics: on the one hand, larger pores continued to develop; and on the other hand, the number of small pores increased due to fragmentation.

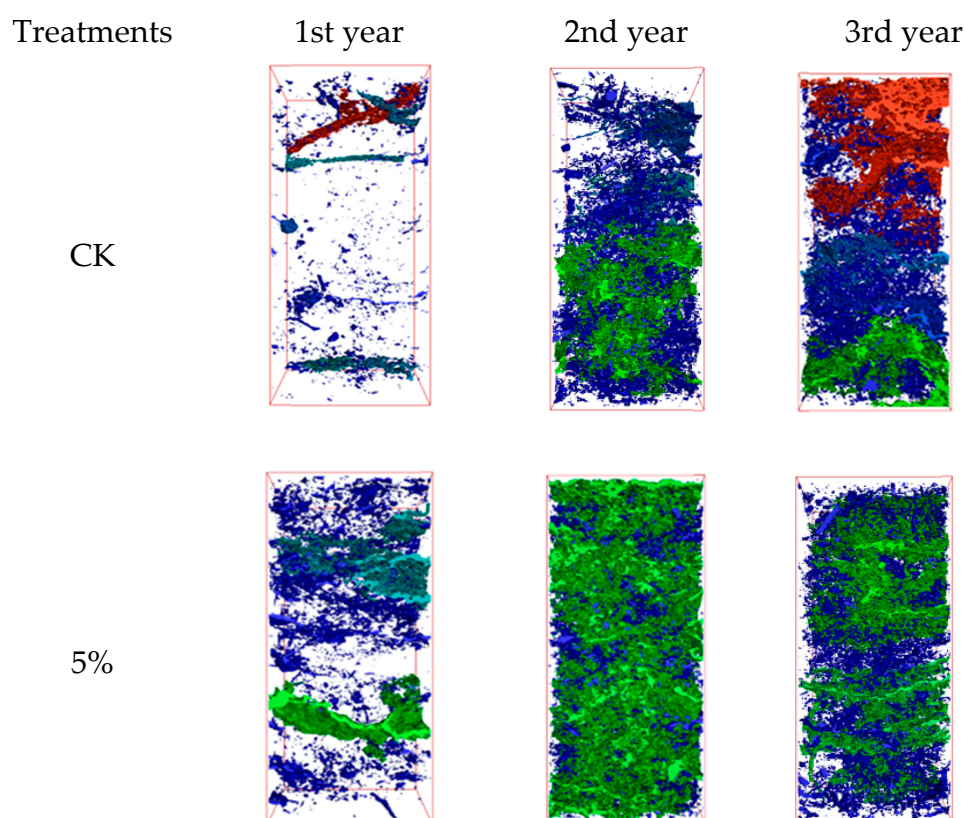


**Figure 6.** Three-dimensional pore structure of reclaimed cambisol treated with 5% weathered coal humic acid treatment.

## 4. Discussion

### 4.1. Influence of Weathered Coal Humic Acid on Distribution and Stability of Soil Aggregates

Using (>0.25 mm) water-stable aggregate content to evaluate the stability of soil aggregates can reflect the improvement of soil structure (Figure 6). In this study, the weathered coal humic acid changed the size distribution of water-stable aggregates, increased the content of water-stable macroaggregates, and decreased that of water-stable microaggregates and silt and clay. The reason may be that weathered coal humic acid is rich in  $-COOH$ ,  $-CO$ ,  $-CO-O-C-$ ,  $-OH$ , and other oxygen-containing functional groups [16], which has chemical properties such as hydrophilicity, complexation, ion exchange, and physical properties such as adsorption and colloid. It combined with soil clay minerals to form organic-inorganic complexes, which could increase the content of water-stable soil aggregates. In addition, the activated preparation of weathered coal sulfonated-

humic acid C can provide organic energy for soil microorganisms [17] and has a high ability to enhance biological activity [18]. After entering the soil, it can promote agglomeration, enhance the cementation between soil particles, and improve stability of soil structure. Messiga et al. [19] believed that the slow turnover rate of large aggregates resulted in high organic C content in large aggregates. In addition, the strong bond formed by organic C binding with soil minerals reduces the availability of organic C to microorganisms [20] and significantly reduces the organic C mineralization rate of large aggregates [21]; the above conclusions were similar to our conclusions.

The research showed that both weathered coal significantly increased soil total organic carbon, particulate and mineral-bound organic carbon ( $P < 0.05$ ). There were no significant differences in soil total organic carbon content. Weathered Coal increased the soil organic carbon content in all aggregate fractions. While the Weathered Coal improved the soil aggregate stability [22]. The reason could be the characteristics of Weathered Coal. While it has high cation exchange capacity, which increases its potential of “binding” agent for soil matter and minerals [23]. Due to its complex structure and many branch chains, small soil particles have a stronger ability to be formed large aggregates [24].

The MWD and GMD values are important evaluation indexes for stability of soil aggregates, reflecting the increase in the content of macroaggregates. In this experiment, the MWD and GMD of soil aggregates were significantly affected by humic acid application amount, but not by year, with 5% treatment the largest. And addition of weathered coal humic acid promoted the formation of water-stable macroaggregates ( $>0.25$  mm) at year 1, and water-stable macroaggregates disintegrated at year 2 to form water-stable microaggregates (0.053–0.25 mm). The silt and clay ( $<0.053$  mm) were dispersed in water-stable microaggregates in year 3. Biochar improved MWD and GMD values of soil aggregates and the proportion of macroaggregates, and improved the stability of aggregates. The soil aggregate stability increased with the increase of biochar application in a certain range [25]. This result was similar with our conclusions. It would be related to our application of weathered coal humic acid. Organic amendment facilitated aggregate stability, as exogenous organic matter directly or indirectly provides the binding agents for soil aggregation [26]. Studies have shown that when soil aggregates are moistened by water, the air in pores is compressed and expands, resulting in disintegration of large aggregates into microaggregates, and then the silt and clay in the microaggregates will be dispersed and broken, while humic acid has high permeability reduction and water retention performance [27]. This can slow the wetting rate of soil water and improve stability of soil aggregates.

#### *4.2. Influence of Weathered Coal Humic Acid on Organic C of Aggregates of Different Sizes*

The organic C content in soil aggregates is affected by fertilization, amendments, and other factors. In this study, application of weathered coal humic acid in reclaimed cambisol increased the content of organic C in water-stable microaggregates and silt and clay; the content of organic C in silt and clay for the 5% treatment was significantly higher than for CK. In the study of Huang et al. [28], mycelium existing in large aggregates cemented some stable biochar particles, and the organic C content increased in these aggregates was mostly the inert C source of biochar itself. At the same time, large aggregates contain more humus and other substances, which also affect the organic C content [26]. Although the added exogenous organic C differs, both can increase the content of organic C in aggregates by means of mycelium and humic acid existing in large aggregates. The difference is that humic acid of weathered coal can significantly change the fraction distribution of aggregates while biochar does not.

Because the balance between decomposition and accumulation of organic C depends on the availability of substrates and the microbial transformation process affected by environmental conditions [29,30] and whether soil microbial products can be stably stored in soil determines the level of organic C accumulation [31–33]. In this study, addition of weathered coal humic acid increased the POC and MOC contents, with the increase related to the age and application amount, consistent with results of Beatrice et al. [34]. The addition of exogenous organic C can increase soil POC content; for instance, Yu et al. [35] found that continuous addition of glucose increased the MOC

content. On the one hand, there are many unfilled adsorption sites in MOC, and low molecular weight organic C such as glucose will be protected by binding with minerals. On the other hand, POC is considered a prerequisite for formation of MOC, and soil POC may be transformed into MOC. This may be related to the difference in exogenous organic C. Glucose is easily soluble in water, while weathered coal is a mineral source of humic acid, which plays an important role in the transformation and stability of soil organic matter through biological processing and transformation [36].

#### 4.3. Influence of Weathered Coal Humic Acid on Soil Pore Structure

Soil pore structure network and its availability determine the distribution, diffusion, and transport of soil moisture and nutrients, and are of great significance for the abundance, movement, and distribution of soil animals and microorganisms [37,38]. Soil pores are generally classified according to their equivalent diameter, and can be divided into storage pores  $<30\ \mu\text{m}$ , capillary pores  $30\text{--}100\ \mu\text{m}$ , and macropores  $>100\ \mu\text{m}$  [39]. Peng et al. [40] believe that soil utilization will destroy or reduce soil pores, reduce soil porosity, and rupture elongated pores. This is similar to this study. In this study, weathered coal humic acid affected pore distribution and shape in soil, and the equivalent diameter of soil pores was divided into three categories:  $30\text{--}75$ ,  $75\text{--}100$ , and  $>100\ \mu\text{m}$ . Most of the soil pores were macropores with  $>100\ \mu\text{m}$ . This may be related to the year-by-year addition of weathered coal humic acid. On the one hand, the humic acid acts as the “cementing agent” of mineral particles to form microaggregates, reducing the number of small pores; on the other hand, it affects the composition and community structure of soil microorganisms, increasing their activity, and making soil pore structure more complex [41].

Soil pore shape reflects the regularity of soil pores and affects soil water conservancy characteristics. In this study, irregular pores were the main type, followed by regular, and then fine pores. With time, fine porosity increased and regular porosity decreased, similar to previous research [42]. Long-term cultivated soil is dominated by elongated pores, followed by irregular, and then regular pores. The proportion of elongated pores decreases with increased cultivation time, while regular and irregular pores show an opposite trend, unlike our study, probably because the humic acid promoted the accumulation of organic C, resulting in the formation of complex soil pore structure dominated by elongated pores. Our experiment was a 3-year field micro-plot experiment conducted on raw soil, while Peng et al. [42] conducted a long-term fertilizer experiment on cropland soil with high fertility. So, the pore structure of the cropland soil is more complex.

Compared with CK treatment of macroaggregates, the total porosity of the biochar treatment increased, while the numbers of independent pores decreased and of connected pores increased [43], similar to our results. In our studies, addition of weathered coal humic acid for 3 years significantly increased the porosity, independent pore number, and average pore volume of reclaimed cambisol compared with CK, the pore number and connected pore number were positively correlated with time, and the independent pore number and average pore number volume reached maxima at year 2. The reason may be that the weathered coal humic acid better promoted development of soil pores than biochar. The average pore volume and connectivity reached maxima at year 2, and then some robust macropores were broken, average pore volume decreased, pore number and independent pore number increased, and the connectivity decreased.

## 5. Conclusions

It is advisable to have addition of 5% weathered coal humic acid in reclaimed cambisol.

In reclaimed cambisol, addition of weathered coal humic acid promoted the formation of water-stable macroaggregates ( $>0.25\ \text{mm}$ ) at year 1, and this class of aggregates had the highest content. The water-stable macroaggregates disintegrated at year 2 to form water-stable microaggregates ( $0.053\text{--}0.25\ \text{mm}$ ), and then water-stable microaggregates had the highest content. The silt and clay ( $<0.053\ \text{mm}$ ) were dispersed in water-stable microaggregates in year 3, the content of silt and clay was the highest, and the content of the 5% treatment was the highest of all years. The MWD and GMD were greatest and the soil structure was the most stable for the 5% treatment at year 3. Soil TOC content increased with time and application amounts, and the organic C content of water-stable aggregates

increased with increased application. The highest content was in silt and clay (<0.053 mm) for years 1 and 2, and the highest aggregate fraction content was in soil TOC and water-stable microaggregates for year 3 under 5% treatment (0.053–0.25 mm). At year 3, POC and MOC of the 5% treatment ranged within 6.17–16.05 and 7.62–15.58 g/kg, respectively, with the largest aggregate fraction being silt and clay (<0.053 mm).

For year 1 of the 5% treatment, independent pores dominated; at year 2, the number of pores decreased slightly, but average pore volume increased, forming robust connected pores; and at year 3, some pores were broken, the number of elongated and irregular pores increased, and irregular pores reached 75.27%. The number of  $P_{30-75\mu\text{m}}$  pores decreased with time, while the number of  $P_{75-100\mu\text{m}}$  and  $P_{>100\mu\text{m}}$  increased. In year 3, the number of  $P_{30-75\mu\text{m}}$  pores was 21.9% and of  $P_{75-100\mu\text{m}}$  and  $P_{>100\mu\text{m}}$  pores was 19.7% and 58.4%, respectively.

**Author Contributions:** Methodology and original draft preparation were conducted by X.D; Conceptualization, review, funding acquisition and supervision were performed, W.F.; editing of the manuscript and validation, data curation were carried out by Q.M.; writing—review and editing, supervision, project administration were carried out by F.L. and G.W.; All authors have read and agreed to the published version of the manuscript.

**Funding:** This research was funded by a project supported by National Natural Science (U1710255-4).

**Data Availability Statement:** The original contributions presented in the study are included in the article/supplementary material, further inquiries can be directed to the corresponding author/s.

**Conflicts of Interest:** The authors declare no conflict of interest.

## References

1. Anna, Y.; Yakov, K. Dual nature of soil structure: The unity of aggregates and pores. *Geoderma* **2023**, 434.
2. Zhang, W.; Li, S.; An, T.; zhu, P.; Xu, Y.; Peng, C.; Liu, X.; Wang, J. Advances in Research on Relationships Between Soil Pore Structure and Soil Microenvironment and Organic Carbon Turnover. *Journal of Soil and Water Conservation* **2019**, 33, 1-9.
3. Kravchenko, A.N.; Guber, A.K. Soil pores and their contributions to soil carbon processes. *Geoderma* **2017**, 287, 31-39.
4. Dhaliwal, J.K.; Kumar, S. 3D-visualization and quantification of soil porous structure using X-ray microtomography scanning under native pasture and crop-livestock systems. *Soil & Tillage Research* **2022**, 1-8.
5. Li, B.; Zhou, H.; Wang, G.; Liu, G.; Gao, W.; Zhu, K.; Chen, C. Explore the “Transparent” Soils : Soilporelogy Has Sailed. *Acta Pedologica Sinica* **2023**, 60, 1221–1230.
6. Feng, Y.; Wang, J.; Bai, Z.; Reading, L. Effects of surface coal mining and land reclamation on soil properties: A review. *Earth-Science Reviews* **2019**, 191, 12-25.
7. Reynolds, B.; Reddy, K. Infiltration rates in reclaimed surface coal mines. *Water, Air, & Soil Pollution* **2012**, 223, 5941-5958.
8. Ahirwal, J.; Maiti, S.K.; Singh, A.K. Changes in ecosystem carbon pool and soil CO<sub>2</sub> flux following post-mine reclamation in dry tropical environment, India. *Science of The Total Environment* **2017**, 583, 153-162.
9. Yan, L.; Ya-fu, T.; Yue-chao, Y.; Yuan-mao, J.; Dongdong, C. Effects of large-grained activated humic acid fertilizer on soil aggregates and organic carbon in apple orchard soil. *Chinese Journal of Applied Ecology* **2022**, 33, 1021–1026.
10. Zhanbin, H.; Junyi, F.; Haoran, M.; Meiling, W. Effects of humic acid on soil improvement and water and fertilizer use efficiency in dryland agriculture. *Agricultural Research in the Arid Areas* **2023**, 41, 49-54.
11. Shiping, W.; Meng, W.; Pengfa, L.; Jia, L.; Guilong, L.; Kai, L.; Ming, L.; Zhongpei, L. Effects of Humic Acid on Fungal Community Structure in a Peanut-continuous Cropping Soil. *Acta Pedologica Sinica* **2023**, 60, 846-856.
12. Yeasmin, S.; Singh, B.; Johnston, C.T.; Hua, Q.; Sparks, D.L. Changes in particulate and mineral-associated organic carbon with land use in contrasting soils. *Pedosphere* **2023**, 33, 421-435.
13. Wenzhao, L.; Hu, Z.; Xiaomin, C.; Xinhua, P.; Xichu, Y. Characterize of aggregate microstructures of paddy soil under different patterns of fertilization with synchrotron on radiation micro-CT. *Acta Pedologica Sinica* **2014**, 51, 67-74.
14. Zhao, D.; Xu, M.; Liu, G.; Ma, L.; Zhang, S.; Xiao, T.; Peng, G. Effect of vegetation type on microstructure of soil aggregates on the Loess Plateau, China. *Agriculture, Ecosystems and Environment* **2017**, 242.

15. Zhou, H.; Peng, X.; Peth, S.; Xiao, T.Q. Effects of vegetation restoration on soil aggregate microstructure quantified with synchrotron-based micro-computed tomography. *Soil and Tillage Research* **2012**, *124*, 17-23.
16. Krumins, J.; Yang, Z.; Zhang, Q.; Yan, M.; Klavins, M. A study of weathered coal spectroscopic properties. *Energy Procedia* **2017**, *128*, 51-58.
17. Zhou, R.; Tian, J.; Cui, Z.; Zhang, F. Microbial necromass within aggregates atabilizes physically-protected c response to cropland management. *Frontiers of Agricultural Science and Engineering* **2023**.
18. Ranran, Z.; Yuan, L.; Zhao, B.; Li, Y.; Lin, Z. Structural characteristics of humic acids derived from Chinese weathered coal under different oxidizing conditions. *PLoS One* **2019**, *14*, 0217469.
19. Messiga, A.J.; Ziadi, N.; Angers, D.A.; Morel, C.; Parent, L.-E. Tillage practices of a clay loam soil affect soil aggregation and associated C and P concentrations. *Geoderma* **2011**, *164*, 225-231.
20. Rakhsh, F.; Golchin, A.; Beheshti Al Agha, A.; Nelson, P.N. Mineralization of organic carbon and formation of microbial biomass in soil: Effects of clay content and composition and the mechanisms involved. *Soil Biology and Biochemistry* **2020**, *151*, 108036.
21. Liu, Z.K.W.; Lal, W.L.R.; Dang, Y.P.; Zhao, X.; Zhang, H. Mechanisms of soil organic carbon stability and its response to no-till: A global synthesis and perspective. *Glob Chang Biol* **2022**, *28*, 693-710.
22. Zhang, X.; Zheng, J.; Wang, K.; Wang, X.; Zhang, Z.; Xie, X.; Cai, J. Greater mineral and aggregate protection for organic carbon in the soil amended by weathered coal than by biochar: Based on a 3-year field experiment. *Geoderma* **2023**, *438*, 116639.
23. Marousek, J.; Vochozka, M.; Plachy, J.; Zak, J. Glory and misery of biochar. *Clean Technologies & Environmental Policy* **2017**, *19*, 311-317.
24. Weil, R.R.; Brady, N.C. *The Nature and Properties of Soils*. ; Pearson: 2017.
25. Sun, Q.; Meng, J.; Lan, Y.; Shi, G.; Yang, X.; Cao, D.; Chen, W.; Han, X. Long-term effects of biochar amendment on soil aggregate stability and biological binding agents in brown earth. *CATENA* **2021**, *205*, 105460.
26. Six, J.; Bossuyt, H.; Degryze, S.; Denef, K. A history of research on the link between (micro)aggregates, soil biota, and soil organic matter dynamics. *Soil & Tillage Research* **2004**, *79*.
27. LE BISSONNAIS, Y. Aggregate stability and assessment of soil crustability and erodibility: I. Theory and methodology. *European Journal of Soil Science* **1996**, *47*, 425-437.
28. Huang, R.; Lan, M.; Liu, J.; Gao, M. Soil aggregate and organic carbon distribution at dry land soil and paddy soil: the role of different straws returning. *Environ Sci Pollut Res Int* **2017**, *24*, 27942-27952.
29. Buckeridge, K.M.; Creamer, C.; Whitaker, J. Deconstructing the microbial necromass continuum to inform soil carbon sequestration. *Functional Ecology* **2022**, *36*, 1396-1410.
30. Jílková, V.; Jandová, K.; Sim, A.; Thornton, B.; Paterson, E. Soil organic matter decomposition and carbon sequestration in temperate coniferous forest soils affected by soluble and insoluble spruce needle fractions. *Soil Biology and Biochemistry* **2019**, *138*, 107595.
31. Chen, J.; Seven, J.; Zilla, T.; Dippold, M.A.; Blagodatskaya, E.; Kuzyakov, Y. Microbial C:N:P stoichiometry and turnover depend on nutrients availability in soil: A <sup>14</sup>C, <sup>15</sup>N and <sup>33</sup>P triple labelling study. *Soil Biology and Biochemistry* **2019**, *131*, 206-216.
32. Čapek, P.; Choma, M.; Tahovská, K.; Kaňa, J.; Kopáček, J.; Šantrůčková, H. Coupling the resource stoichiometry and microbial biomass turnover to predict nutrient mineralization and immobilization in soil. *Geoderma* **2021**, *385*, 114884.
33. Cui, J.; Zhu, Z.; Xu, X.; Liu, S.; Jones, D.L.; Kuzyakov, Y.; Shibistova, O.; Wu, J.; Ge, T. Carbon and nitrogen recycling from microbial necromass to cope with C:N stoichiometric imbalance by priming. *Soil Biology and Biochemistry* **2020**, *142*, 107720.
34. Giannetta, B.; Plaza, C.; Galluzzi, G.; Benavente-Ferraces, I.; García-Gil, J.C.; Panettieri, M.; Gascó, G.; Zaccone, C. Distribution of soil organic carbon between particulate and mineral-associated fractions as affected by biochar and its co-application with other amendments. *Agriculture, Ecosystems & Environment* **2024**, *360*, 108777.
35. Yu, Q.; Zhang, Z.; He, Y.; Ming, H.; Wang, G.; Dun, X.; Wu, Q.; Gao, P. Secondary shrubs promoted the priming effect by increasing soil particle organic carbon mineralization. *Frontiers in Forests and Global Change* **2023**, *6*.
36. Wu, S.; Konhauser, K.O.; Chen, B.; Huang, L. "Reactive Mineral Sink" drives soil organic matter dynamics and stabilization. *npj Materials Sustainability* **2023**, *1*, 3.

37. Hampton, H.G.; Watson, B.N.J.; Fineran, P.C. The arms race between bacteria and their phage foes. *Nature* **2020**, *577*, 327-336.
38. N, U.; Nielsen. *Global to local scales* Cambridge University Press: Cambridge, 2019.
39. Liu, Y.; Shi, Z.; Yin, J.; Lin, W. Analysis of Soil Water Characters Between Upland Red Soil and Paddy Soil. *Journal of Soil and Water Conservation* **2009**, *23*, 232-235.
40. Peng, J.; Wu, X.; Ni, S.; Wang, J.; Song, Y.; Cai, C. Investigating intra-aggregate microstructure characteristics and influencing factors of six soil types along a climatic gradient. *CATENA* **2022**, *210*, 105867.
41. Xia, Q.; Zheng, N.; Heitman, J.L.; Shi, W. Soil pore size distribution shaped not only compositions but also networks of the soil microbial community. *Applied Soil Ecology* **2022**, *170*, 104273.
42. Jue, P.; QingSong, Y.; ChenYang, Z.; Shimin, N.; Junguang, W.; Chongfa, C. Aggregate pore structure, stability characteristics, and biochemical properties induced by different cultivation durations in the Mollisol region of Northeast China. *Soil & Tillage Research* **2023**, *233*.
43. Liu, J.; Lu, S. Amendment of different biochars changed pore characteristics and permeability of Ultisol macroaggregates identified by X-ray computed tomography (CT). *Geoderma* **2023**, *434*, 116470.

**Disclaimer/Publisher's Note:** The statements, opinions and data contained in all publications are solely those of the individual author(s) and contributor(s) and not of MDPI and/or the editor(s). MDPI and/or the editor(s) disclaim responsibility for any injury to people or property resulting from any ideas, methods, instructions or products referred to in the content.